Supporting information

Molecular surface modification of silver chalcogenolate clusters

Lei Hu,[a] Ming-Ming Sheng,[a] Shun-Shun Qin,[a] Hua-Tian Shi,[a] Maria Strømme,[b] Qian-Feng Zhang,*[a] Chao Xu*[ab]

[a] Institute of Molecular Engineering and Applied Chemistry, Anhui University of Technology, Ma'anshan, 243002, P. R. China. chao.xu0203@outlook.com; zhangqf@ahut.edu.cn

[b] Department of Materials Science and Engineering, Uppsala University, The Ångström Laboratory, Box 35, 751 03 Uppsala, Sweden. chao.xu@angstrom.uu.se

Table S1. Synthesis parameter for **1−7**.

SCC	Silver thiolate precursor	Solvent	Ligand	yield
1	$(^{i}PrSAg)_n$ (18.3 mg, 0.1 mmol)	1.5 mL CH_3CN/1.5 mL MeOH	DMAc (87.0 mg, 1.0 mmol)	53.0%
2	$(^{i}PrSAg)_n$ (18.3 mg, 0.1 mmol)	1.5 mL CH_3CN 1.5 mL MeOH	2,3-Me_2Py(54.0 mg, 0.5 mmol)	60.6%
3	$(^{i}PrSAg)_n$ (18.3 mg, 0.1 mmol)	1.5 mL CH_3CN 1.5 mL MeOH	2-EtPy (107.0 mg, 1.0 mmol)	34.9%
4	$(EtSAg)_n$ (16.9 mg, 0.1 mmol)	3.0 mL THF	2-EtPy (107.0 mg，1.0 mmol)	44.3%
5	$(EtSAg)_n$ (16.9 mg, 0.1 mmol)	3.0 mL THF	2,4-Me_2Py (54.0 mg, 0.5 mmol)	80.5%
6	$(^{i}BuSAg)_n$ (19.7 mg, 0.1 mmol)	1.5 mL CH_3CN 1.5 mL MeOH	Py (79.0 mg, 1.0 mmol)	34.2%
7	$(^{t}BuSAg)_n$ (19.7 mg, 0.1 mmol)	3.0 mL CH_3CN	3,5-Me_2Py (54.0 mg, 0.5 mmol)	76.2%

Note: the synthesis avoided the use of toluene (a relatively low volatile co-solvent used for the synthesis of reported pyridine-protected SCCs [1, 2]), which could accelerate the crystallization process and increase the yield and reproducibility of the synthesis.

X-ray crystallography

The crystallographic data of clusters **1−7** was collected on a Bruker SMART Apex 2K CCD diffractometer using graphite-monochromated Mo-$K\alpha$ radiation (λ = 0.71073 Å) at 296 K. Data reduction and absorption correction were performed by STINT [3] and SADABS[4] software, respectively. The crystal structure was solved by the direct method using a SHELXS software package.[5,6] All non-hydrogen atoms were refined anisotropically. **5** includes disordered solvent molecules of THF. PLATON/SQUEEZE [7] was used to remove the electron density of disordered solvent molecules and to calculate approximately solvent accessible void space in the unit cell. Table S2 summarizes the crystallographic data and experimental details for **1−7**.

Table S2. Crystal data and structure refinement details of cluster **1**-**7**

Compound	**1**	**2**	**3**
Molecular formula	$C_{54}H_{96}N_6O_{18}F_{18}S_6Ag_{12}$	$C_{72}H_{96}O_{12}N_6F_{18}S_6Ag_{12}$	$C_{72}H_{96}O_{12}N_6F_{18}S_6Ag_{12}\cdot 2H_2O$
Formula weight	2946.16	3066.34	3102.38
Crystal system	trigonal	trigonal	monoclinic
Space group	*R -3 m*	*R -3*	*P 21/n*
a (Å)	16.8860(10)	27.392(4)	15.995(5)
b (Å)	16.8860(10)	27.392(4)	17.314(6)
c (Å)	28.799(3)	11.302(3)	18.391(6)
α (°)	90	90	90
β (°)	90	90	90
γ (°)	120	120	90
V (Å^3)	7111.4(12)	7344(2)	5093(3)
Z	3	3	2
ρ (g cm^{-1})	2.070	2.080	2.023
μ (mm^{-1})	1.839	2.558	2.462
F(000)	4284	4464	3016
T/K	296(2)	296(2)	296(2)
*R*1, w*R*2 [$I>2\sigma(I)$]	0.0467, 0.1321	0.0286, 0.0725	0.0387, 0.0983

Compound	**4**	**5**	**6**	**7**
Molecular formula	$C_{66}H_{84}O_{12}N_6F_{18}S_6Ag_{12}$	$C_{66}H_{84}O_{12}N_6F_{18}S_6Ag_{12}\cdot C_4H_8O$	$C_{66}H_{82}O_{12}N_6F_{18}S_6Ag_{12}\cdot 4H_2O$	$C_{78}H_{108}O_{12}N_6F_{18}S_6Ag_{12}$
Formula weight	2982.19	3054.29	3052.24	3150.50
Crystal system	Trigonal	trigonal	Monoclinic	Orthorhombic
Space group	*R -3*	*R -3*	*P21/n*	*Cmca*
a (Å)	21.113(10)	20.625(5)	11.933(3)	29.633(14)
b (Å)	21.113(10)	20.625(5)	28.031(8)	18.580(9)
c (Å)	18.108(9)	40.283(9)	15.304(4)	19.796(10)
α (°)	90	90	90	90
β (°)	90	90	98.596(4)	90
γ (°)	120	120	90	90
V (Å^3)	6990(7)	14840(8)	5061(2)	10900(9)
Z	3	6	2	4
ρ (g cm^{-1})	2.125	2.002	2.003	1.920
μ (mm^{-1})	2.685	2.533	2.477	2.301
F(000)	4320	8874	2956	6144
T/K	296(2)	296(2)	296(2)	296(2)
*R*1, w*R*2 [$I>2\sigma(I)$]	0.0394, 0.1121	0.0316, 0.0838	0.0566, 0.1551	0.0286, 0.0672

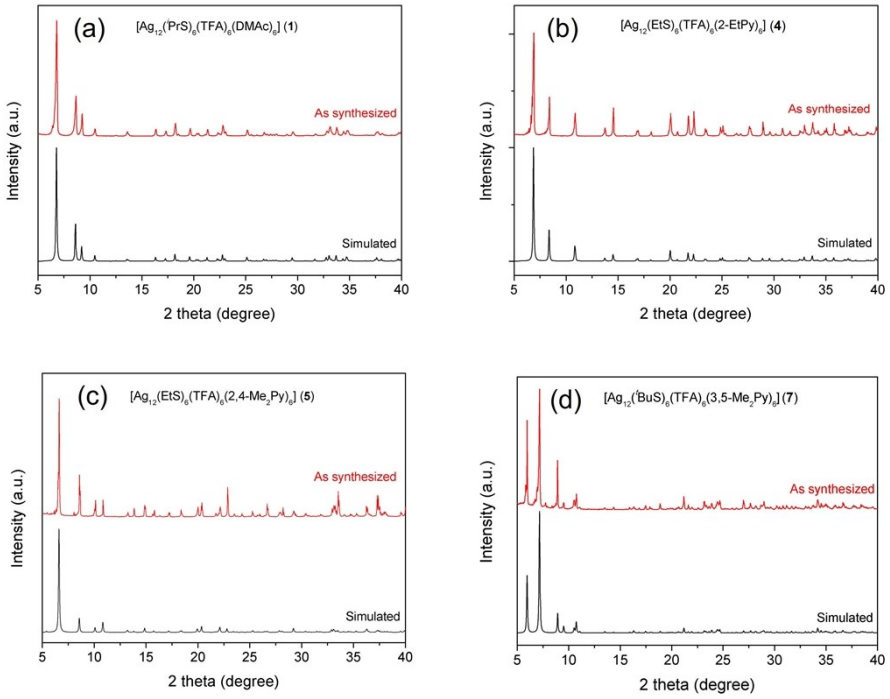

Fig. S1 Simulated and experimental XRD patterns of (a) $[Ag_{12}(^{i}PrS)_6(TFA)_6(DMAc)_6]$ (**1**), (b) $[Ag_{12}(EtS)_6(TFA)_6(2\text{-}EtPy)_6]$ (**4**), (c) $[Ag_{12}(EtS)_6(TFA)_6(2,4\text{-}Me_2Py)_6]$ (**5**), and (d) $[Ag_{12}(^{t}BuS)_6(TFA)_6(3,5\text{-}Me_2Py)_6]$ (**7**).

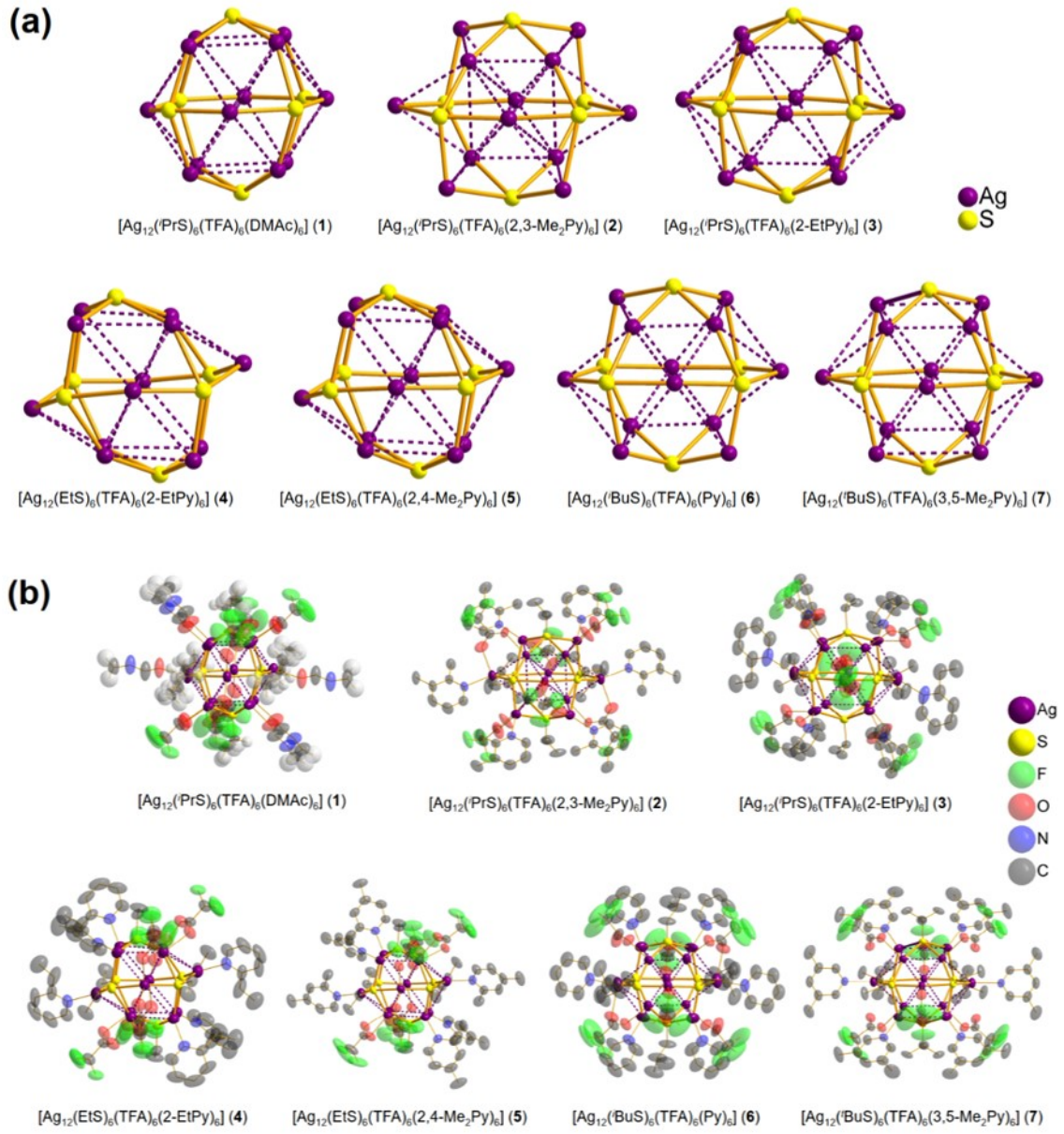

Fig. S2 (a) Crystal structure of the $[Ag_{12}S_6]$ cores in clusters **1-7**; (b) crystal structure of the clusters **1-7** showing the thermal ellipsoids at the 50% probability level.

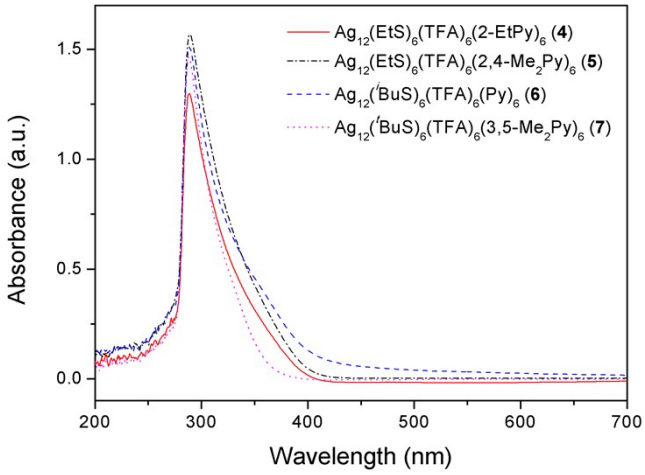

Fig. S3 Solution UV-vis absorption spectra of $[Ag_{12}(EtS)_6(TFA)_6(2\text{-}EtPy)_6]$ (**4**) (solvent: DMF, concentration: 6.71×10^{-5} M), $[Ag_{12}(EtS)_6(TFA)_6(2,4\text{-}Me_2Py)_6]$ (**5**) (solvent: CH_3CN, concentration: 4.00×10^{-5} M), $[Ag_{12}(^{t}BuS)_6(TFA)_6(Py)_6]$ (**6**) (solvent: DMF, concentration: 5.13×10^{-5} M), and (d) $[Ag_{12}(^{t}BuS)_6(TFA)_6(3,5\text{-}Me_2Py)_6]$ (**7**) (solvent: CH_3CN, concentration: 4.12×10^{-5} M).

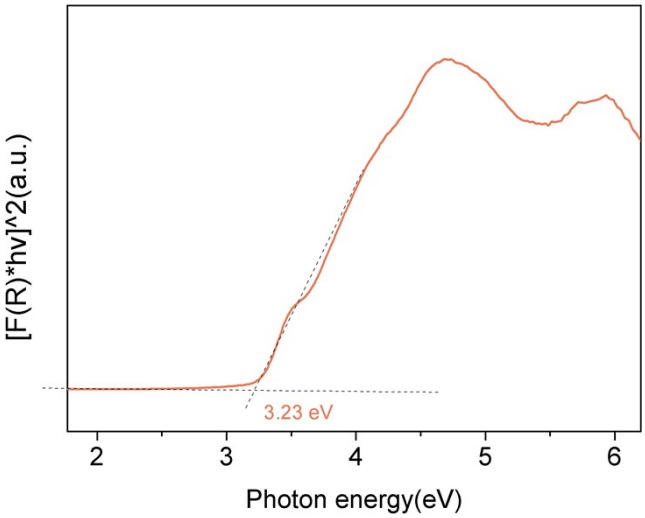

Fig. S4 Calculation of band gap of $[Ag_{12}(EtS)_6(TFA)_6(2,4\text{-}Me_2Py)_6]$ (**5**) from its solid UV-vis absorption spectrum by using Kubelka-Munk function.

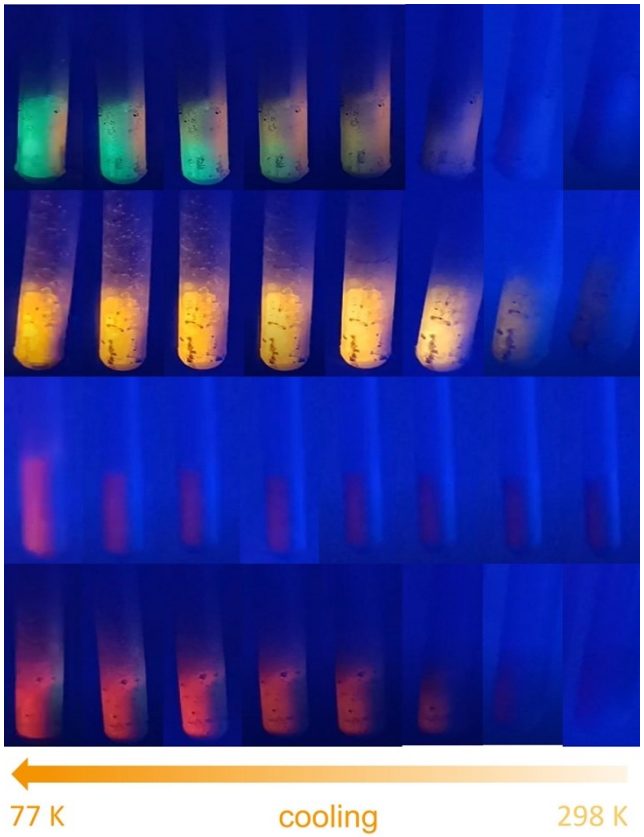

Fig. S5 Digital images showing the temperature dependent luminescence emission of the SCCs under UV light irradiation (λ = 365 nm) (from top to bottom: $[Ag_{12}(EtS)_6(TFA)_6(2,4\text{-}Me_2Py)_6]$ (**5**), $[Ag_{12}(^tBuS)_6(TFA)_6(3,5\text{-}Me_2Py)_6]$ (**7**), $[Ag_{12}(^tBuS)_6(TFA)_6(Py)_6]$ (**6**), $[Ag_{12}(EtS)_6(TFA)_6(2\text{-}EtPy)_6]$ (**4**)).

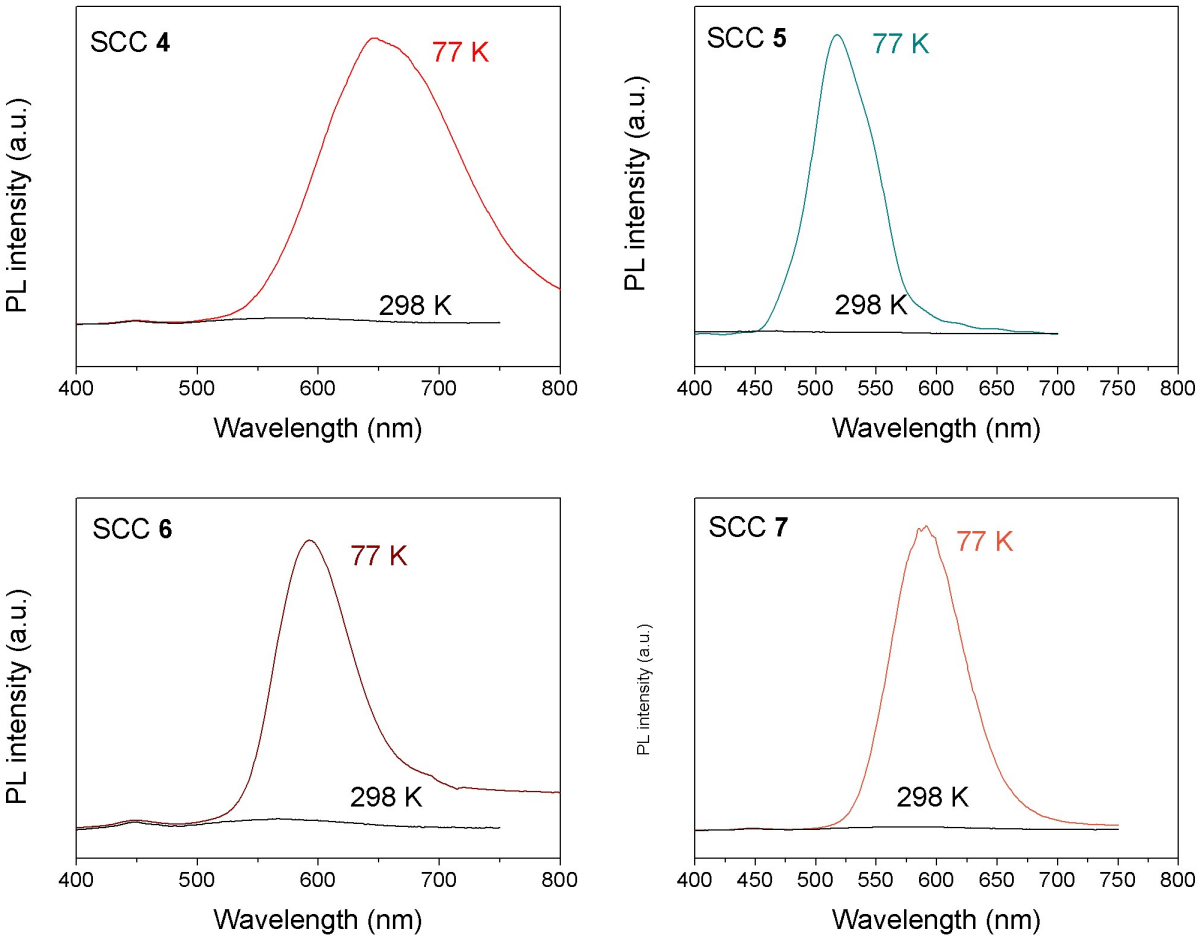

Fig. S6 Luminescence emission spectra of SCCs $[Ag_{12}(EtS)_6(TFA)_6(2\text{-}EtPy)_6]$ (**4**) (λ_{ex} = 350 nm), $[Ag_{12}(EtS)_6(TFA)_6(2,4\text{-}Me_2Py)_6]$ (**5**) (λ_{ex} = 360 nm), $[Ag_{12}(^{i}BuS)_6(TFA)_6(Py)_6]$ (**6**) (λ_{ex} = 350 nm), and $[Ag_{12}(^{t}BuS)_6(TFA)_6(3,5\text{-}Me_2Py)_6]$ (**7**) (λ_{ex} = 350 nm) in solid state recorded at 298 K and 77 K.

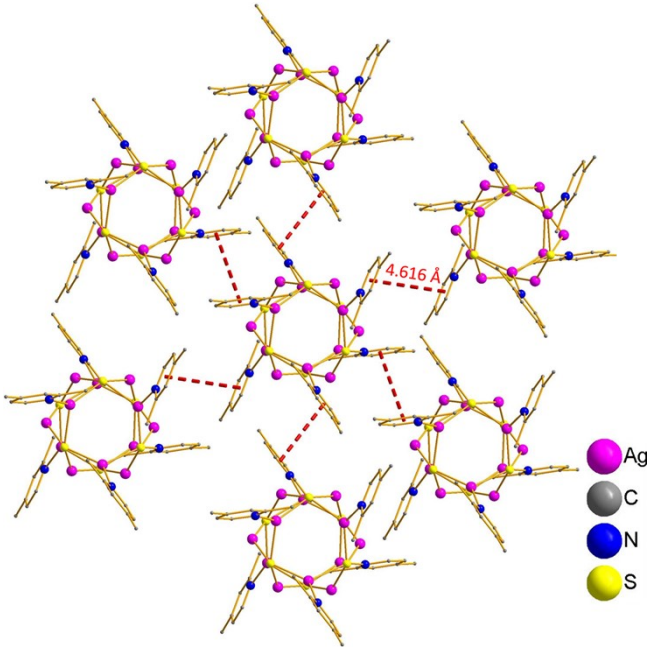

Fig. S7 Intermolecular π-π stacking between the adjacent pyridine rings in $[Ag_{12}(EtS)_6(TFA)_6(2,4\text{-}Me_2Py)_6]$ (**5**).

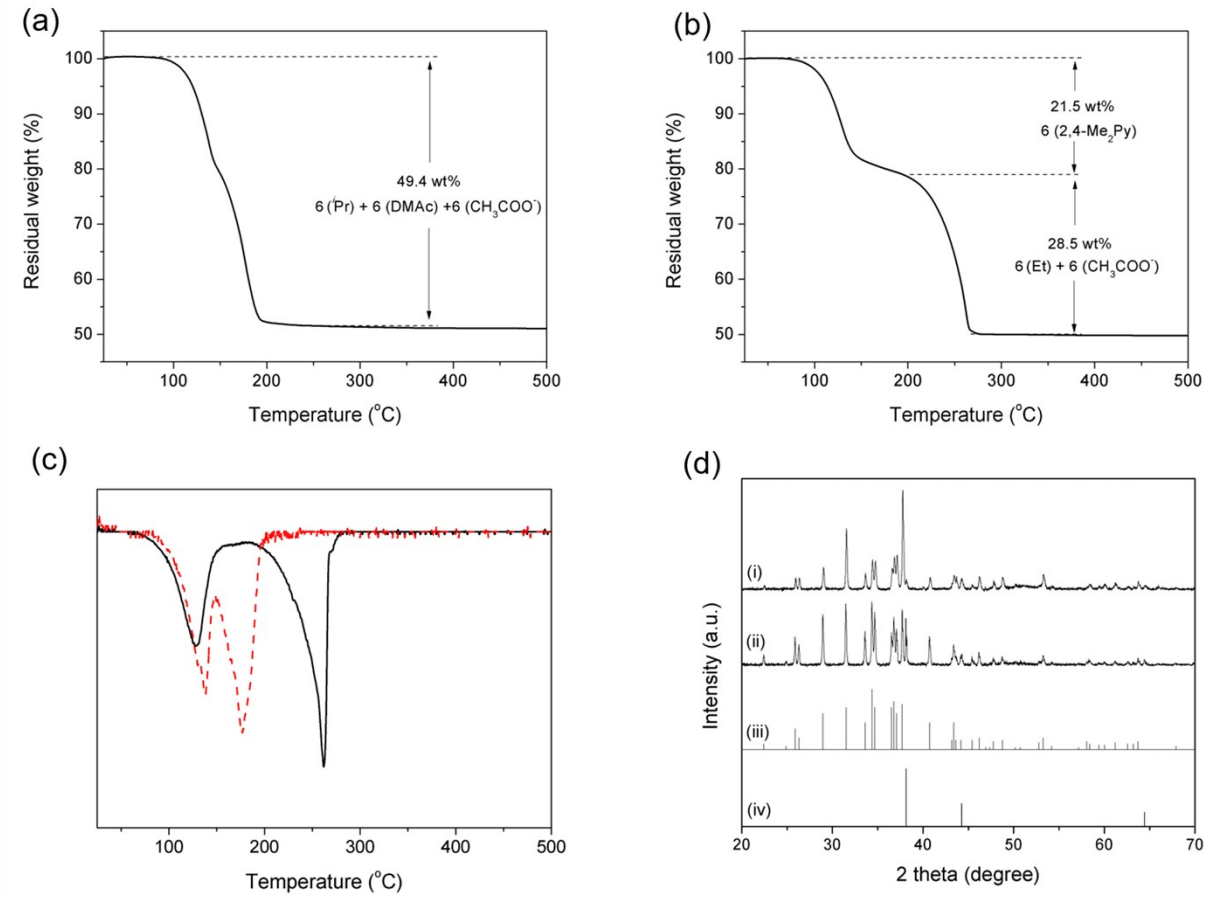

Fig. S8 Thermogravimetric analysis curves of (a) $[Ag_{12}(^{i}PrS)_6(TFA)_6(DMAc)_6]$ (**1**) and (b) $[Ag_{12}(^{i}PrS)_6(TFA)_6(2\text{-}EtPy)_6]$ (**3**) under a N_2 atmosphere; (c) First derivative curves of the TGA results displaying the onset decomposition temperatures of **1** (dashed line) and **3** (solid line). (d) Powder X-ray diffraction (XRD) patterns of the pyrolyzed residue of cluster **1** (i) and cluster **3** (ii), and standard XRD patterns of the pure Ag_2S (ICDD reference code: 00-014-0072) (iii) and Ag (ICDD reference code: 00-004-0783) (iv).

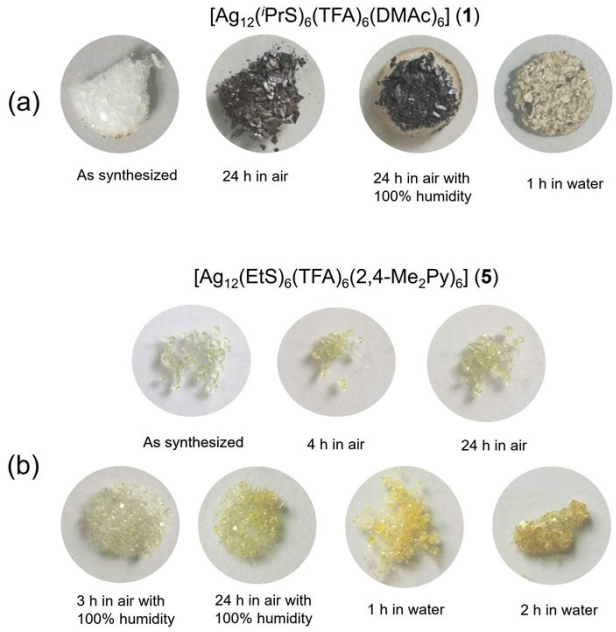

Fig. S9 Optical images of (a) $[Ag_{12}(^{i}PrS)_6(TFA)_6(DMAc)_6]$ (**1**) and (b) $[Ag_{12}(EtS)_6(TFA)_6(2,4\text{-}Me_2Py)_6]$ (**5**) in different environments.

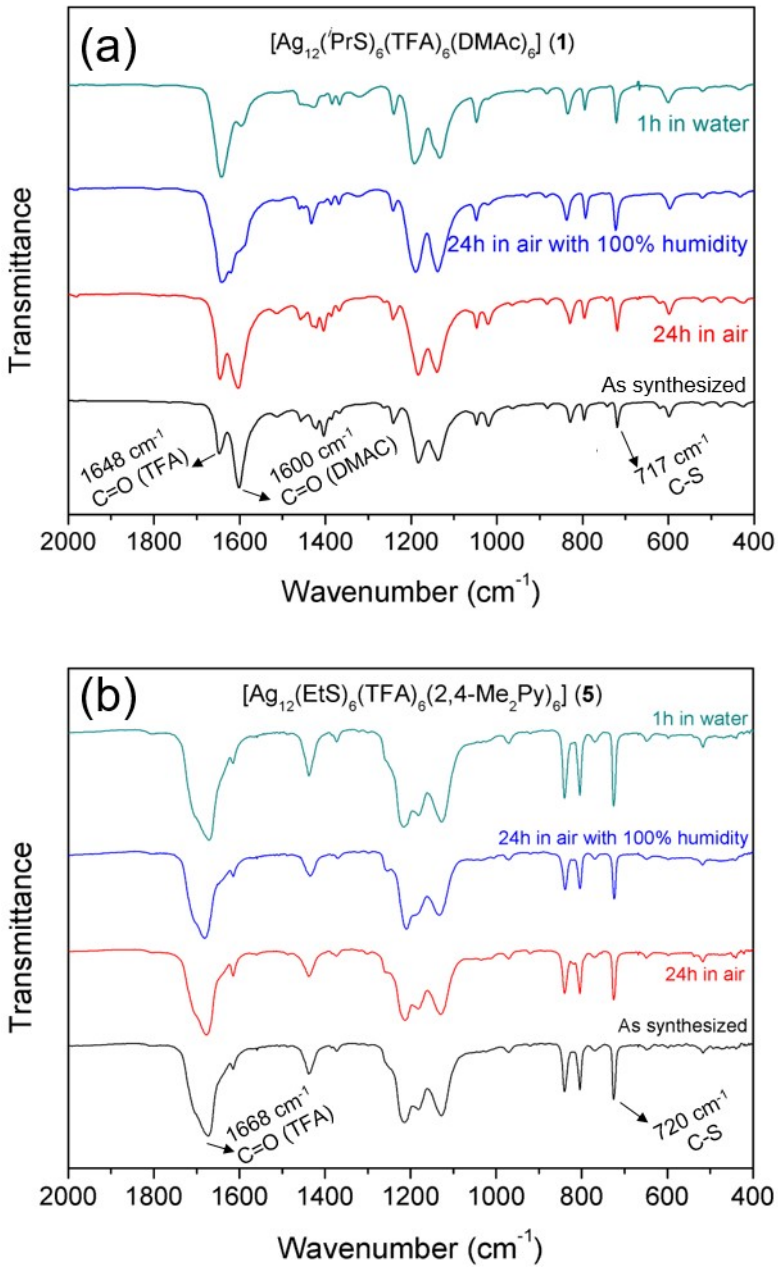

Fig. S10 Infrared spectra of (a) $[Ag_{12}(^{i}PrS)_6(TFA)_6(DMAc)_6]$ (**1**) and (b) $[Ag_{12}(EtS)_6(TFA)_6(2,4\text{-}Me_2Py)_6]$ (**5**) in different environments (from bottom to top: as synthesized, and after storage in ambient air for 24 h, in air at 100% humidity for 24 h, and in water for 1 h).

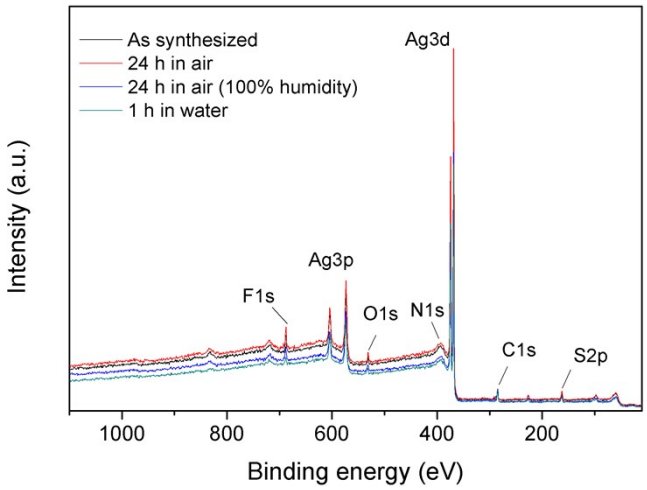

Fig. S11 Survey XPS spectra of $Ag_{12}(EtS)_6(TFA)_6(2,4\text{-}Me_2Py)_6]$ (**5**) in different environments.

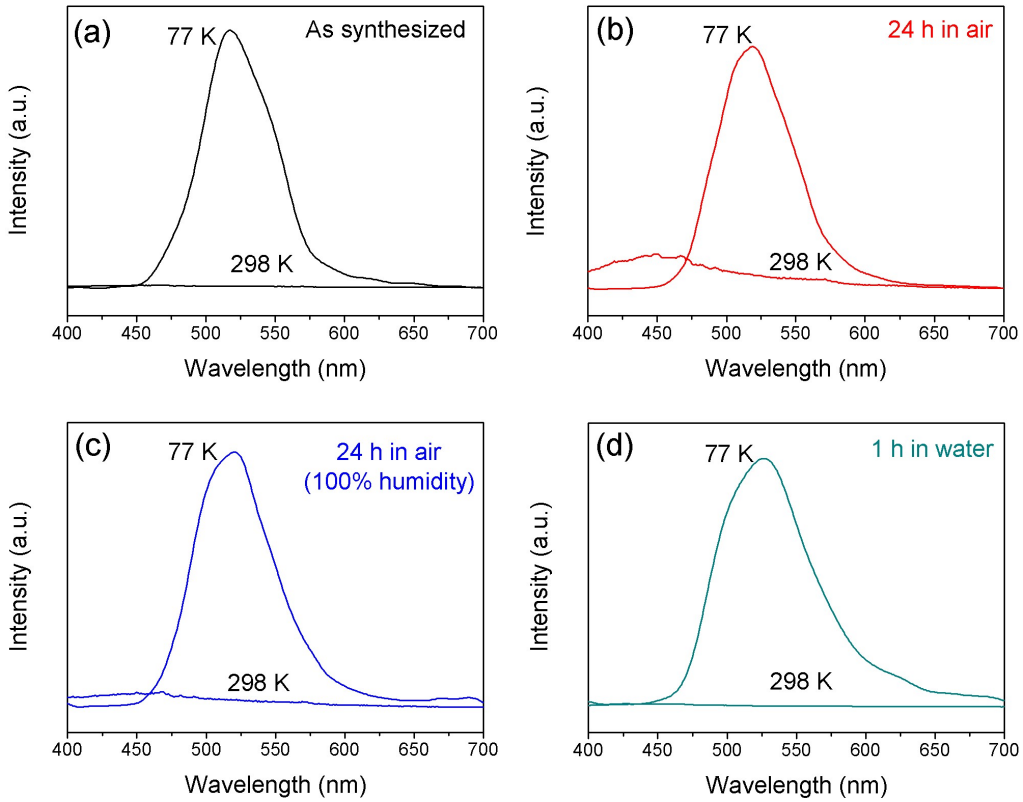

Fig. S12 Luminescence emission spectra of $[Ag_{12}(EtS)_6(TFA)_6(2,4\text{-}Me_2Py)_6]$ (**5**) in solid state recorded at 298 K and 77 K (excited at 360 nm). (a) as synthesized; (b) after storage in ambient air for 24 h, (c) in humid air for 24h, and (d) in water for 1 h.

References:

[1] Y.-L. Li, W.-M. Zhang, J. Wang, Y. Tian, Z.-Y. Wang, C.-X. Du, S.-Q. Zang and T. C. W. Mak, *Dalton Trans.*, **2018**, *47*, 14884.

[2] Y.-L. Shen, J.-L. Jin, Y.-P. Xie and X. Lu, *Dalton Trans.*, **2020**, *49*, 12574.

[3] SAINT (Version 6.02a), Bruker Bruker AXS Inc., Madison, Wisconsin, USA, **1998**.

[4] G. M. Sheldrick, SADABS, University of Göttingen, Germany, **1996**.

[5] G. M. Sheldrick, *Acta Crystallogr., Sect. A,* **2008**, *64*, 112.

[6] G. M. Sheldrick. *Acta Crystallogr., Sect. C*, **2015**, *71*, 3.

[7] A. L. Spek, *Acta Cryst*., **2009**, *D65*, 148-155